Int. J. Electrochem. Sci., 12 **(2017)** 7249 – 7261, doi: 10.20964/2017.08.25

International Journal of
ELECTROCHEMICAL
SCIENCE
www.electrochemsci.org

N,N-diethyl-trimethylsilylamine as an Electrolyte Additive for Enhancing Electrochemical Performance of High Voltage Spinel Cathode

Jiahui Chen[1,2,3], *Fuxiao Liang*[1], *Hui Zhang*[1], *Jianhong Liu*[1], *Cuihua Li*[1,*]

[1] College of Chemistry and Environmental Engineering, Shenzhen University, Shenzhen 518060, China
[2] Shenzhen Institutes of Advanced Technology, Chinese Academy of Sciences, Shenzhen 518055, China
[3] Shenzhen College of Advanced Technology, University of Chinese Academy of Sciences, Shenzhen 518055, China
[*]E-mail: licuihuasz@163.com

Received: 3 May 2017 / *Accepted:* 31 May 2017 / *Published:* 12 July 2017

In this work, N,N-diethyl-trimethylsilylamine (EMSA) is used as an electrolyte additive for a 5 V-class high voltage $LiNi_{0.5}Mn_{1.5}O_4$ cathode. In presence of 0.5 wt.% EMSA, Li/$LiNi_{0.5}Mn_{1.5}O_4$ cell exhibits an attractive cycling performance compared to the cell without EMSA, improving the discharge capacity retention from 76.1 % to 84.9% after 500 cycles at 1 C and 25 °C, and from 52.4% to 94.8% after 100 cycles at 0.5 C and 55 °C. ^{19}F nuclear magnetic resonance (^{19}F NMR), inductively coupled plasma atomic emission spectrometry (ICP-AES) and X-ray photoelectron spectroscopy (XPS) studies reveal that EMSA serves as a hydrofluoric acid scavenger to alleviate the dissolution of Mn and Ni ions from $LiNi_{0.5}Mn_{1.5}O_4$ cathode and the concurrent decomposition of electrolyte. As a result, the stability of the cathode/electrolyte interface and cycling performance of $LiNi_{0.5}Mn_{1.5}O_4$ are significantly improved. Moreover, the superior cycling performance of a Li/graphite cell with EMSA is also achieved because the surface film modified by EMSA allows facile charge transfer.

Keywords: Lithium ion battery, Electrolyte additive, N,N-diethyl-trimethylsilylamine, High voltage, Spinel $LiNi_{0.5}Mn_{1.5}O_4$

1. INTRODUCTION

Spinel $LiNi_{0.5}Mn_{1.5}O_4$ is considered to be a promising cathode material for advanced lithium ion batteries used in electronic devices and has a higher energy density due to its moderate specific

capacity of 147 mAh g^{-1} and its high operating voltage of approximately 4.7 V vs. Li/Li^+ [1-4]. However, the interfacial instability between electrode and electrolyte under high voltage conditions that gives rise to the substantial decomposition of the standard carbonate-based electrolyte is a major challenge for the practical application of this high voltage $LiNi_{0.5}Mn_{1.5}O_4$ cathode [5-7]. Moreover, the $LiPF_6$ salt that is commonly used in the standard electrolyte is susceptible to heat and trace water [8, 9]. The thermal decomposition of $LiPF_6$ at elevated temperature produces a highly active acid, PF_5, which is an initiator for electrolyte decomposition [10]. Sloop et al. [11] demonstrated that PF_5 can catalyze the ring-opening polymerization of ethylene carbonate and lead to the production of a poly(ethylene oxide)-like polymer. It is important to note that trace amounts of water readily cause hydrolysis of $LiPF_6$ and then generate HF, facilitating electrolyte decomposition and promoting transition metal ion dissolution from the cathode [12, 13]. The HF and other phosphoric acid products (HPO_2F_2, H_2PO_3F, H_3PO_4) generated by the hydrolysis reaction of $LiPF_6$ severely consume active Li^+ to form LiF and $Li_xPF_yO_z$-type compounds [14-16]. These inorganic lithium salts tend to precipitate on the cathode surface and contribute to the formation of a resistive solid electrolyte interface (SEI) film [17, 18]. It is believed that the abovementioned aggressive reactions are responsible for the large irreversible capacity loss and distinct capacity fading of the $LiNi_{0.5}Mn_{1.5}O_4$ cathode.

Extensive research has been conducted to prevent the defects induced by $LiPF_6$, with a focus on finding electrolyte components that are suitable for high voltage cathodes. Fluorinated ethers and carbonates [19], sulfones [20], dinitriles [21], and ionic liquids [22] combining new types of lithium salts [23-26], such as lithium difluoro(oxalate)borate, lithium bis(trifluoromethanesulfonyl)imide and lithium bis(fluorosulfonyl)imide, have been proposed for the development of high voltage electrolyte systems. Additionally, electrolyte additives with the function of stabilizing $LiPF_6$ have been used to enhance the cycling capability of various cathode materials. Pieczonka et al. [27] reported that a lithium bis(oxalate)borate additive can stabilize the carbonate-based electrolyte by scavenging the PF_5 that is generated by the thermal decomposition of $LiPF_6$. As a result, electrolyte decomposition and HF generation were suppressed, which in turn resulted in a better cycling performance of the $LiNi_{0.42}Fe_{0.08}Mn_{1.5}O_4$ cathode. Hisayuki et al. [28] demonstrated that plausible acid derived from the reaction of $LiPF_6$ with water causes capacity fading of $Li_{1.01}Mn_{1.99}O_4$ at 80 °C. Surprisingly, an improved cycling performance of the cathode was achieved after the electrolyte was dehydrated and acid-neutralized by hexamethyldisilazane. Li et al. [29] reported that heptamethyldisilazane can be combined with HF to form a stable compound in the electrolyte, leading to an enhanced storage stability and cycling performance of the $Li/LiMn_2O_4$ cell. Recently, Song et al. [16] carried out a comparative study by using some phosphite-based additives, including triphenyl phosphite, trimethyl phosphite, tris(2,2,2-trifluoroethyl) phosphite, and tris(trimethylsilyl) phosphite in $Li/LiNi_{0.5}Mn_{1.5}O_4$ cells. Their investigation revealed that these additives are efficient for mitigating the hydrolysis of $LiPF_6$, for eliminating HF from the electrolyte and for creating a protective SEI film on $LiNi_{0.5}Mn_{1.5}O_4$ cathode, thus obtaining a drastically improved cycling performance of $Li/LiNi_{0.5}Mn_{1.5}O_4$ cells at 60 °C.

Herein, N,N-diethyl-trimethylsilylamine (EMSA) was used as an electrolyte additive to remove HF from the carbonate-based electrolyte and to improve the cycling performances of high voltage $LiNi_{0.5}Mn_{1.5}O_4$ cathodes at room and elevated temperatures. Electrochemical techniques and an ex-situ analysis were conducted to understand the role of EMSA in the enhanced performance of the

Li/$LiNi_{0.5}Mn_{1.5}O_4$ cell. Furthermore, the impact of EMSA on the electrochemical performance of a graphite anode was also explored.

2. EXPERIMENTAL

Battery grade ethylene carbonate (EC), ethyl methyl carbonate (EMC), diethyl carbonate (DEC) and lithium hexafluorophosphate ($LiPF_6$) were kindly provided by Optimum Nano Energy Co. Ltd. EMSA was purchased from Adamas and used without further treatment. A blank electrolyte with a composition of 1 M $LiPF_6$-EC/EMC/DEC (3/5/2 in volume) was prepared. EMSA (0.5 wt.%) was added into the blank electrolyte to obtain the additive-containing electrolyte. The water and HF contents of these electrolytes were controlled to less than 15 ppm. A $LiNi_{0.5}Mn_{1.5}O_4$ electrode with an active material loading of approximately 1.6 mg cm^{-2} was prepared by using a mixture of 80 wt.% $LiNi_{0.5}Mn_{1.5}O_4$ (Shenzhen Tianjiao Co. Ltd.), 10 wt.% acetylene carbon black and a 10 wt.% polyvinylidene fluoride (PVDF) binder dissolved in N-methyl-2-pyrrolidone. The resulting slurry was cast on aluminum foil, followed by overnight drying in a convection oven at 70 °C. The coated foil was punched into 14-mm diameter round discs and dried again at 110 °C under vacuum for 8 h. A graphite electrode was also prepared by coating a slurry of 80 wt.% artificial graphite (Shenzhen Kejing Co. Ltd.), 10 wt.% acetylene carbon black and 10 wt.% PVDF on copper foil. CR2032 coin-type half cells were fabricated with a $LiNi_{0.5}Mn_{1.5}O_4$ cathode or graphite anode as the working electrode, lithium sheet as the counter electrode, Celgard 2400 membrane as the separator and as-prepared electrolyte in a highly pure argon-filled glove box (Unilab, Mbraun) with less than 0.1 ppm of either oxygen or moisture. Identical electrolyte amounts of 50 μL were used for each cell.

Galvanostatic charge/discharge tests of Li/$LiNi_{0.5}Mn_{1.5}O_4$ cells were carried out at 0.1 C (1 C=147 mA g^{-1}) for the initial three cycles between 3.5 and 5 V using a LAND battery test system (CT2001A, Wuhan Land Electronics Co. Ltd.). Then, the cells were cycled at a current of 1 C at 25 °C and 0.5 C at 55 °C, respectively. Li/graphite cells were also galvanostatically cycled at 0.1 C (1 C=372 mA g^{-1}) for three formation cycles and 0.5 C for the remaining cycles between 0.01 and 3 V at 25 °C. Cyclic voltammetry was measured on electrochemical workstation (1470E, Solartron) between 3.5 and 5.0 V with a scan rate of 0.1 mV s^{-1}. Electrochemical impedance spectroscopy (EIS) was performed on a potentiostat (1470E, Solartron) coupled with a frequency response analyzer (FR 1260A, Solartron) at the open-circuit potential with an amplitude of 10 mV. The investigated frequency range was 10^6 Hz to 0.01 Hz for Li/$LiNi_{0.5}Mn_{1.5}O_4$ cells and 10^6 Hz to 0.1 Hz for Li/graphite cells.

For surface characterizations, the cycled Li/$LiNi_{0.5}Mn_{1.5}O_4$ and Li/graphite cells were disassembled in a glove box. The $LiNi_{0.5}Mn_{1.5}O_4$ and graphite electrodes were washed three times with anhydrous dimethyl carbonate (DMC) to remove the residual electrolyte components, and the resulting materials were dried in vacuum at 40 °C. The surface morphologies of the electrodes were observed by scanning electron microscopy (SEM, S3400N, Hitachi). X-ray photoelectron spectroscopy (XPS, Quantera-Ⅱ, Ulvac-Phi) was performed with Al Kα (hν=1486.6 eV) radiation under ultrahigh vacuum using a 0.1 eV step and 26 eV pass energy. The binding energy was calibrated by the hydrocarbon C1s line at 284.6 eV.

To investigate the effect of EMSA on HF removal from the electrolyte, 0.2 vol.% water was added to the blank and EMSA-containing electrolytes. The ^{19}F nuclear magnetic resonance (^{19}F NMR) spectra of these electrolytes were recorded on an Agilent spectrometer (VNMRS 400) using KF solution as an external reference. The following experiment was carried out to clarify the dissolution behavior of the transition metal ions from the $LiNi_{0.5}Mn_{1.5}O_4$ cathode. Fresh cathodes were placed into sealed vials with a 500 μL-blank and EMSA-containing electrolytes under argon atmosphere. After storage at 60 °C for 5 days, the amount of the Mn and Ni ions in these electrolytes were measured by inductively coupled plasma atomic emission spectrometry (ICP-AES, Optima 7000DV, Perkin Elmer).

3. RESULT AND DISCUSSION

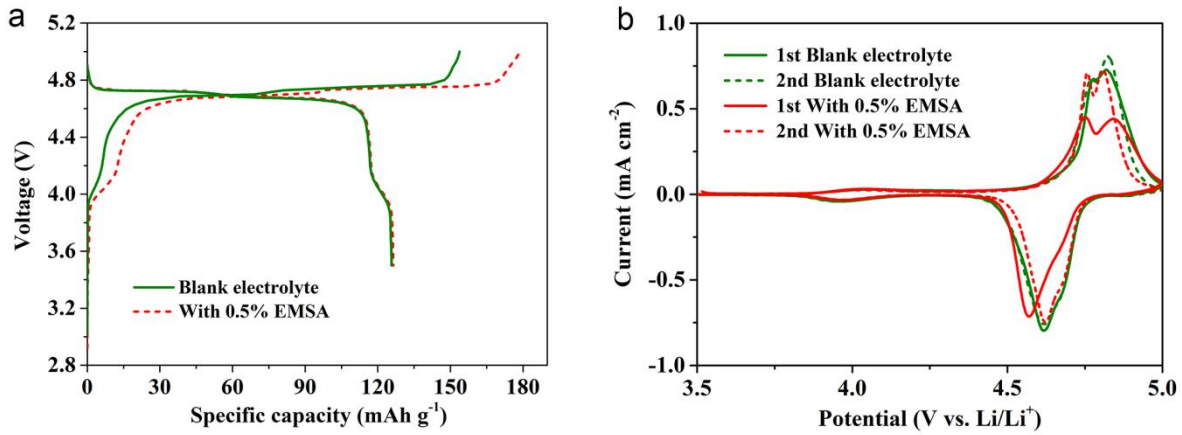

Figure 1. Initial charge/discharge curves (a) and cyclic voltammograms (b) of Li/$LiNi_{0.5}Mn_{1.5}O_4$ cells using blank electrolyte and an EMSA-containing electrolyte at 25 ºC

Fig. 1a shows the initial charge/discharge curves of $LiNi_{0.5}Mn_{1.5}O_4$ in the electrolyte with and without EMSA at 0.1 C and 25 °C. It is known that the voltage plateau near 4.7 V is due to the Ni^{2+}/Ni^{4+} redox reaction and the small voltage plateau at approximately 4 V represents the Mn^{3+}/Mn^{4+} redox process. The Li/$LiNi_{0.5}Mn_{1.5}O_4$ cell with an EMSA-containing electrolyte shows a similar discharge capacity of 126.4 mAh g^{-1} as that of the blank electrolyte (125.7 mAh g^{-1}). However, the initial charge capacity of the $LiNi_{0.5}Mn_{1.5}O_4$ cathode with EMSA is approximately 25 mAh g^{-1} higher than that of the cathode without the additive. Therefore, the $LiNi_{0.5}Mn_{1.5}O_4$ cathode cycled in an EMSA-containing electrolyte exhibits a reduced Coulombic efficiency of 71% compared to the cathode cycled in the blank electrolyte (82%) in the first cycle. This result may be ascribed to the irreversible reaction caused by EMSA during the first charge process. Cyclic voltammetry was carried out to better understand the electrochemical behaviors of blank and EMSA-containing electrolytes. Fig. 1b presents the cyclic voltammograms of the $LiNi_{0.5}Mn_{1.5}O_4$ cathode in blank and EMSA-containing electrolytes. One pair of redox peaks around 4.7 V is attributed to the oxidation/reduction of nickel in $LiNi_{0.5}Mn_{1.5}O_4$, while the small one at 4 V is associated with the oxidation/reduction of

manganese [7]. In the first cycle, the oxidation current of the EMSA-containing electrolyte starts slightly earlier than the blank electrolyte, and then showing smaller redox current of nickel. This result suggests that EMSA is oxidized preferentially to the blank electrolyte, which is in agreement with Fig. 1a. Interestingly, the subsequent cycle shows better reversibility, i.e. less difference in redox peak potentials, for the cathode in the EMSA-containing electrolyte than that in the blank electrolyte. This improved reversibility may benefit from the high quality SEI film modified by EMSA.

After three formation cycles at 0.1 C rate, the Li/$LiNi_{0.5}Mn_{1.5}O_4$ cells with different electrolytes were cycled at 1 C rate between 3.5 and 5 V. As can be seen in Fig. 2, fast capacity fading is observed in the cell with the blank electrolyte that only exhibits a discharge capacity retention of 76.1% based on the discharge capacity at the 4th cycle. On the contrary, a more stable cycling behavior is achieved with the addition of 0.5% EMSA, delivering a discharge capacity of 109 mAh g^{-1}, with a high capacity retention of 84.9% after 500 cycles. The Coulombic efficiency of the cell with EMSA is slightly more stable than that without EMSA, maintaining above 99% after 35 cycles. It is thought that EMSA is involved in forming a SEI film that effectively reduces the oxidative decomposition of the electrolyte on the $LiNi_{0.5}Mn_{1.5}O_4$ cathode surface.

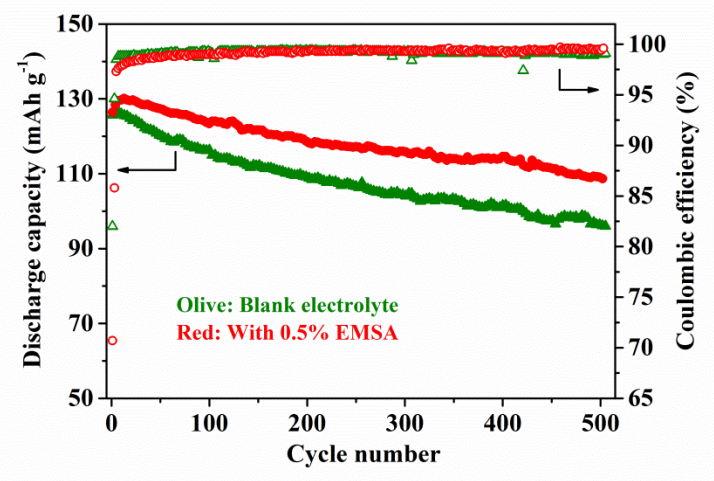

Figure 2. Cycling stability of Li/$LiNi_{0.5}Mn_{1.5}O_4$ cells with blank and EMSA-containing electrolytes under a voltage range of 3.5-5.0 V at 25 °C

Electrochemical impedance spectroscopy was conducted to investigate the effect of EMSA on the cycling performance. The impedance spectra of the Li/$LiNi_{0.5}Mn_{1.5}O_4$ cells with and without the additive measured after 100, 300 and 500 cycles are presented in Figs. 3a and 3b. During charge/discharge cycling, two intersecting semicircles and a sloping tail are observed. According to previous reports [30-33], the semicircle in the high frequency range is related to the surface film resistance on the electrode (R_f), and the semicircle located in the middle frequency range corresponds to the charge transfer resistance between the electrode and electrolyte (R_{ct}). The low frequency straight line is associated with the Li^+ diffusion process in the bulk of the electrode. These spectra are fitted by

using the equivalent circuit model, as shown in the insert in Fig. 3a, and the resultant values are summarized in Table 1.

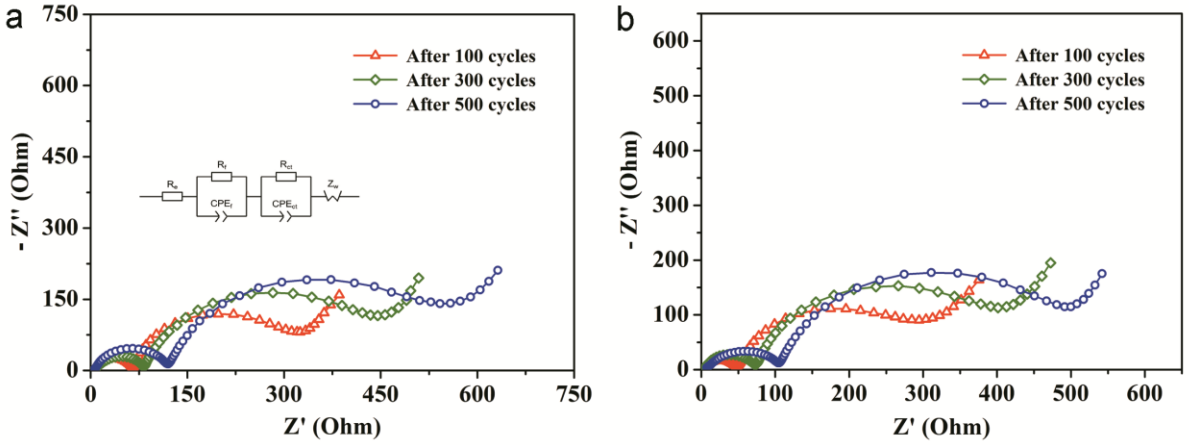

Figure 3. EIS spectra of $Li/LiNi_{0.5}Mn_{1.5}O_4$ cells with a (a) blank electrolyte and (b) EMSA-containing electrolyte during cycling.

Table 1. Fitted results of EIS spectra for $Li/LiNi_{0.5}Mn_{1.5}O_4$ cells

Sample		Blank electrolyte	With 0.5% EMSA
After 100 cycles	R_f (Ω)	61	46
	R_{ct} (Ω)	195	215
After 300 cycles	R_f (Ω)	78	70
	R_{ct} (Ω)	301	316
After 500 cycles	R_f (Ω)	117	105
	R_{ct} (Ω)	383	375

The values of R_f and R_{ct} of the $Li/LiNi_{0.5}Mn_{1.5}O_4$ cells with and without EMSA are comparable as cycling proceeds. In other words, the addition of EMSA is unable to create a less-resistive surface film on the electrode that would facilitate the charge transfer reaction. This implies that the enhanced cycling performance of $LiNi_{0.5}Mn_{1.5}O_4$ bought by EMSA is probably due to the unique function of the EMSA scavenging HF from the electrolyte.

The cycling performances of $Li/LiNi_{0.5}Mn_{1.5}O_4$ cells with different electrolytes were further tested at an elevated temperature of 55 °C and a small rate of 0.5 C, where the unwanted interfacial side reaction between cathode and electrolyte becomes more severe. Fig. 4a clearly shows that the cell with the EMSA additive shows substantial improvement in capacity and cycling stability. A reversible discharge capacity of 120 mAh g^{-1} can be obtained for the cell with an EMSA-containing electrolyte after 100 cycles at 55 °C, corresponding to a capacity retention of 94.8%. In contrast, for the cell with

the blank electrolyte, the discharge capacity continuously decreases from 128.1 mAh g^{-1} to 67.1 mAh g^{-1} over 100 cycles, resulting in an inferior capacity retention of 52.4% (these data are obtained from our previous report and are used for comparison [34]). Moreover, the Coulombic efficiencies of these cells are given in Fig. 4b.

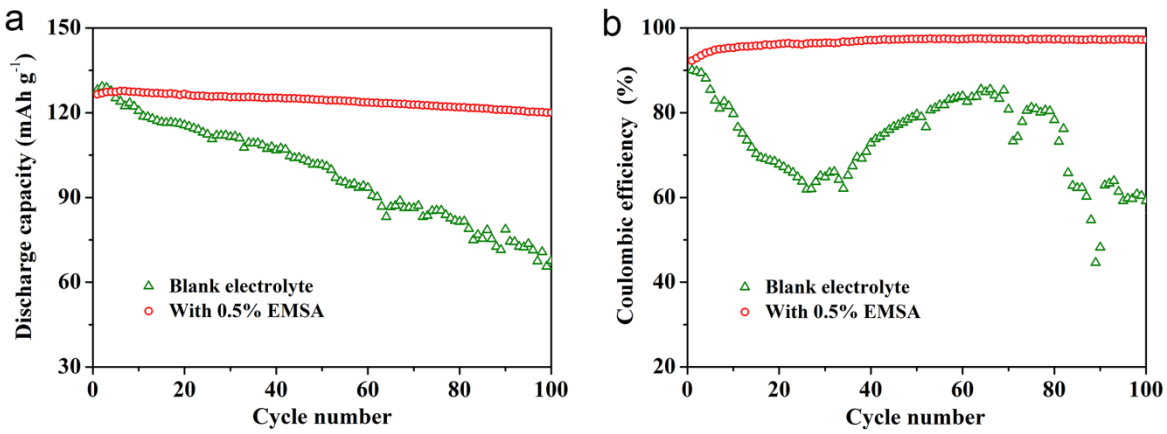

Figure 4. Cycling performances of Li/$LiNi_{0.5}Mn_{1.5}O_4$ cells with blank and EMSA-containing electrolytes at 55 ºC: (a) discharge capacity and (b) Coulombic efficiency

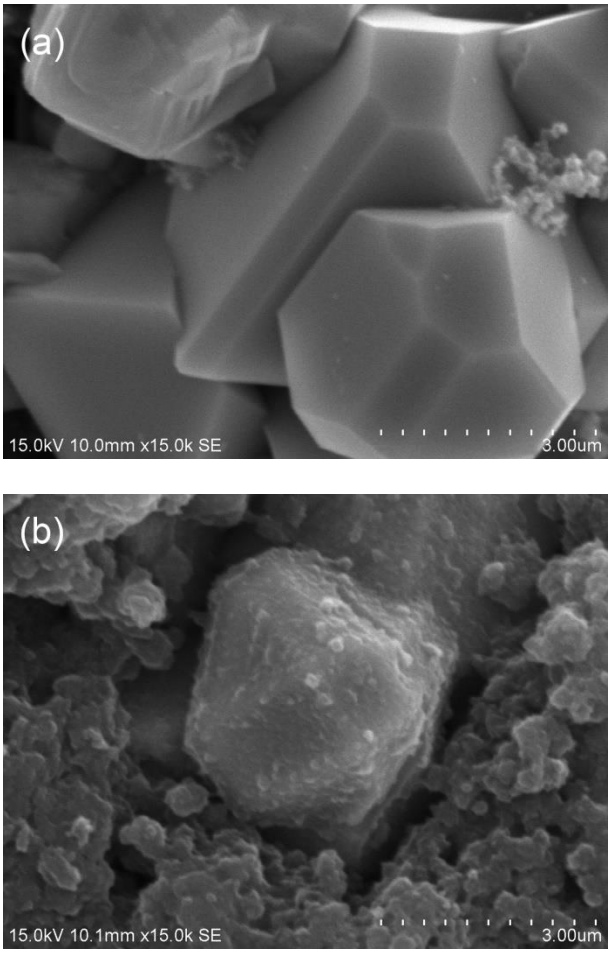

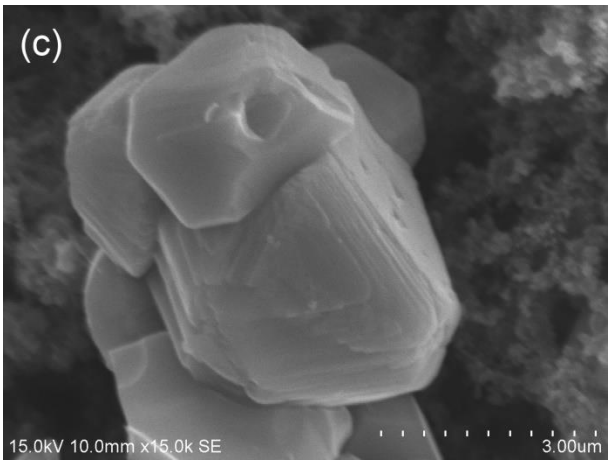

Figure 5. SEM images of $LiNi_{0.5}Mn_{1.5}O_4$ cathodes: (a) fresh cathode, cathodes after 100 cycles in (b) a blank electrolyte and (c) EMSA-containing electrolyte at 55 ºC

A high and stable Coulombic efficiency of over 97% is achieved for the cell with the additive. However, the cell without EMSA shows a very unstable and low Coulombic efficiency. This poor cycling performance may have originated from the following two undesirable reactions: first, the carbonate-based solvent suffers from remarkable decomposition on the $LiNi_{0.5}Mn_{1.5}O_4$ cathode surface under high voltage [5], leading to the formation of a resistive and unstable surface film. Second, the decomposition of $LiPF_6$ at 55 °C becomes more severe and then generates a large HF amount [8]. The increased concentration of HF accelerates the dissolution of transition metal ions from the $LiNi_{0.5}Mn_{1.5}O_4$ cathode. These harmful reactions severely consume the active Li^+ and cause rapid capacity fading of the cell with the blank electrolyte. The substantial improvement in capacity and stability of the cell with an EMSA-containing electrolyte suggests that electrolyte decomposition and metal ion dissolution are greatly alleviated by the use of EMSA as an electrolyte additive under the high voltage and at elevated temperature.

$Li/LiNi_{0.5}Mn_{1.5}O_4$ cells after 100 cycles at 55 °C were disassembled to analyze the surface chemistry of the $LiNi_{0.5}Mn_{1.5}O_4$ cathode.

As shown in Fig. 5a, the surface of the fresh cathode is very clean and smooth. A distinct difference can be observed between the cathodes cycled in blank and EMSA-containing electrolytes at high temperature. It is found that the $LiNi_{0.5}Mn_{1.5}O_4$ cathode cycled in the blank electrolyte is covered with many degradation species (Fig. 5b). The decomposition of the electrolyte concurrently generates species such as lithium alkyl carbonates, polycarbonates and LiF [35]. These products tend to participate in the formation of a resistive SEI film on the cathode surface. However, the cathode cycled in the EMSA-containing electrolyte exhibits a similar morphology to that of the fresh cathode, covering a uniform SEI film (Fig. 5c). This result further confirms that the addition of EMSA effectively suppress the decomposition of the electrolyte and improve the stability of the cathode/electrolyte interface.

XPS was employed to analyze the surface composition of the $LiNi_{0.5}Mn_{1.5}O_4$ cathodes after 100 cycles at 55 °C in blank and EMSA-containing electrolytes, as shown in Fig. 6. The XPS data for the fresh cathode and cathode cycled without EMSA have also been reported by us [34]. The characteristic

peaks of the fresh cathode originated from graphite, the PVDF binder and $LiNi_{0.5}Mn_{1.5}O_4$ and are located at 284.6 eV (C-C), 286.1 eV, 290.9 eV, 688.1 eV (C-F) and 529.7 eV (Metal-O), respectively. In the C1s and O1s spectra, additional peaks associated with C=O (288.7 eV, 531.7 eV) and C-O (286 eV, 533.1 eV), which are the decomposition products of electrolyte components, arise in the cycled cathodes. The intensities of the two peaks obtained from the cathode cycled in the blank electrolyte are relatively stronger than of those of the sample in the EMSA-containing electrolyte, demonstrating that the SEI film modified by EMSA effectively diminishes the oxidative decomposition of the electrolyte.

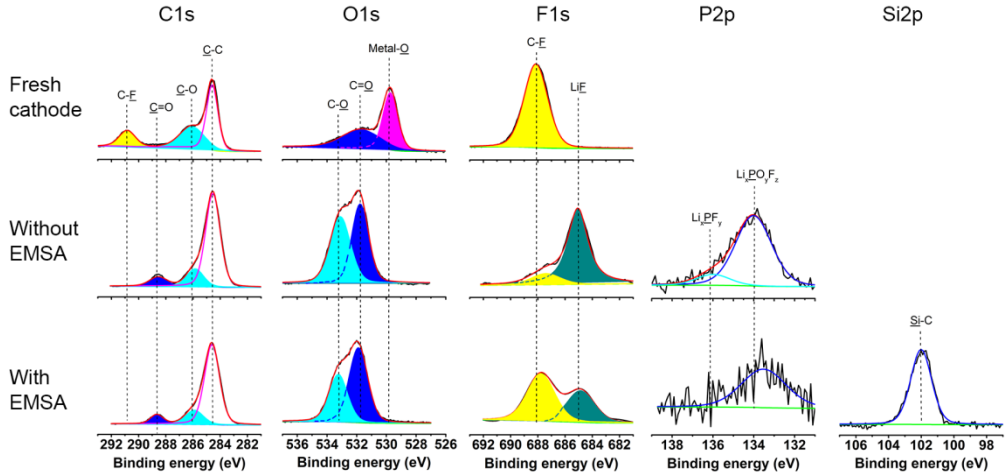

Figure 6. XPS spectra of fresh $LiNi_{0.5}Mn_{1.5}O_4$ cathode and the cathodes after 100 cycles in the electrolyte with and without EMSA at 55 ºC

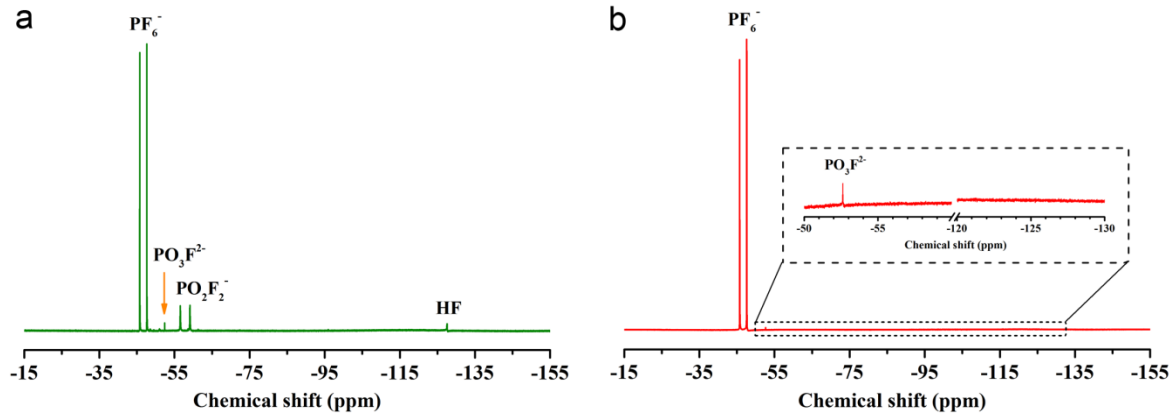

Figure 7. ^{19}F NMR spectra of a (a) blank electrolyte and (b) EMSA-containing electrolyte after the addition of 1 μL of water

In the F1s spectra, the cycled cathodes exhibit two major peaks corresponding to the PVDF binder (687.9 eV) and LiF (684.9 eV). Specifically, the cathode without the additive exhibits a distinctly stronger LiF peak compared to that of the cathodes with EMSA. F1s peak related to PVDF in the cycled cathode with EMSA is stronger than the one without additive, indicating that a thinner SEI film is formed in the presence of EMSA. As for the P2p spectra, a much weaker $Li_xPO_yF_z$ peak can be

seen at the cathode cycled in EMSA-containing electrolyte, while the Li_xPF_y peak is non-detectable. Analysis of the Si2p spectra of the cathode cycled with EMSA shows a characteristic Si-C peak at 102 eV. This organic silicon based compound is likely produced by the reaction between EMSA and HF [36]. The XPS results reveal that the blank electrolyte decomposes more easily at the cathode surface after prolonged cycling at high temperature, covering the surface of $LiNi_{0.5}Mn_{1.5}O_4$ with more resistive decomposition products (such as LiF, $Li_xPO_yF_z$ and Li_2CO_3, etc.). While the HF is eliminated by EMSA, it mitigates the electrolyte decomposition and consequently enhances the stability of the cathode/electrolyte interface.

To understand the function of EMSA in HF removal from the electrolyte, 0.2 vol.% water was added to the blank and EMSA-containing electrolytes, and these electrolytes were then stored at 25 °C for 48 h. The ^{19}F NMR spectra obtained from the resulting electrolytes are presented in Fig. 7. The prominent doublet peak at -45.7 ppm and -47.6 ppm corresponds to the PF_6^- anion. With the addition of a small amount of water, HF and a series of $PO_xF_y^{n-}$ type compounds are produced by the hydrolysis reaction of $LiPF_6$. The three characteristic peaks of these hydrolytic products, as shown in Fig. 7a, from down field to up field are attributed to PO_3F^{2-} (-52.4 ppm), $PO_2F_2^-$ (-56.5 ppm and -59.1 ppm) and HF (-127.6 ppm), respectively. Apparently, the resonances of $PO_2F_2^-$ and HF disappear in the EMSA-containing electrolyte (Fig. 7b). This result indicates that HF in the electrolyte is totally eliminated by EMSA.

Table 2. The amount of Ni and Mn ions in blank and EMSA-containing electrolytes after storage with $LiNi_{0.5}Mn_{1.5}O_4$ at 60 °C

Sample	Mn (ppm)	Ni (ppm)
Blank electrolyte	11.07	3.611
With 0.5% EMSA	4.676	1.642

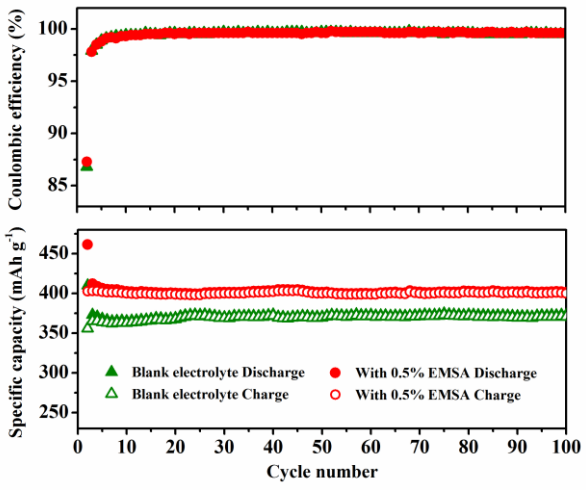

Figure 8. Cycling performances of Li/graphite cells with blank and EMSA-containing electrolytes at 25 ºC

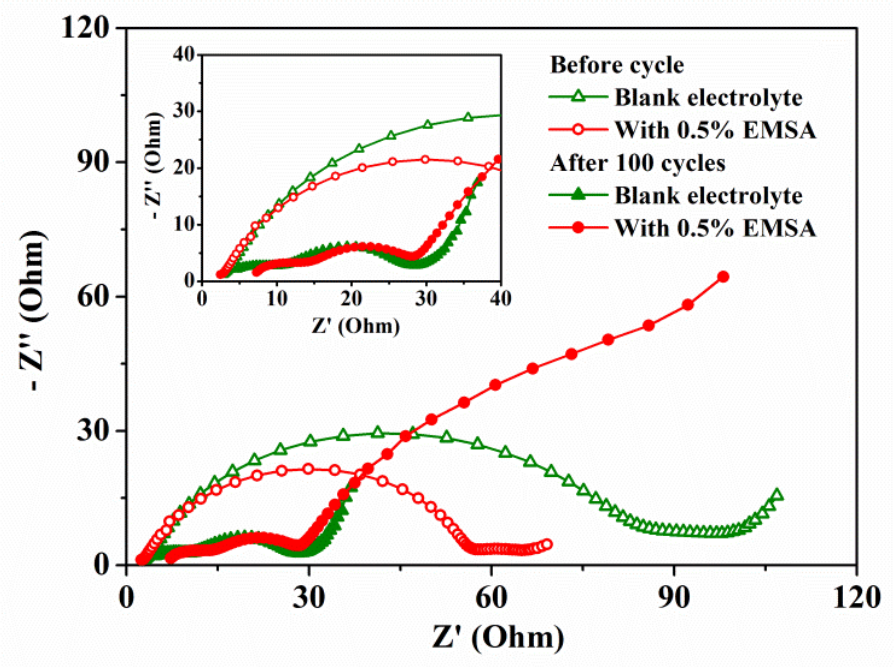

Figure 9. EIS spectra of Li/graphite cells with blank and EMSA-containing electrolytes before cycle and after 100 cycles

As discuss above, HF readily attack the unprotected $LiNi_{0.5}Mn_{1.5}O_4$ cathode and cause transition metal ions dissolution. Table 2 shows that the dissolved amounts of Mn and Ni ions from the fresh cathode stored in EMSA-containing electrolyte decrease by more than half compared to that of stored in blank electrolyte. This suggests that Mn and Ni dissolution are retarded by removing HF from the electrolyte. Thus, this finding provides indirect evidence for the prominent HF scavenging function of EMSA.

Fig. 8 shows the cycling performances of Li/graphite cells in blank and EMSA-containing electrolytes at 25 °C. In the first three cycles, the cells were subjected to a formation cycle at 0.1 C rate and then cycled at 0.5 C rate. Throughout the entire cycling test, the performance of the cell with EMSA is superior to that of the cell without EMSA, delivering a charge capacity of 400 mAh g^{-1} at the 100th cycle. On the other hand, the cell cycled with the blank electrolyte exhibits a charge capacity of only 372.2 mAh g^{-1} after 100 cycles. Due to a large quantity of acetylene carbon black is used in the graphite electrode, the obtained capacity is larger than the calculated capacity of graphite. The Coulombic efficiencies of the Li/graphite cells are maintained close to 100% over 100 cycles, irrespective of the incorporation of EMSA. It is believed that EMSA is beneficial for the enhancement of the cycling performance of the graphite anode by eliminating HF from the electrolyte and consequently stabilizing the anode/electrolyte interface.

Persuasive evidence for the positive impact of EMSA on the improved stability of the anode/electrolyte interface is presented in Fig. 9. The electrochemical impedance spectra of the Li/graphite cells with and without EMSA were measured prior to cycling and after 100 cycles. The graphite anode cycled in the electrolyte with EMSA exhibits a smaller resistance than that cycled in the blank electrolyte prior to cycling and after 100 cycles, indicating that an improved quality of

anode/electrolyte interface constructed by the addition of EMSA allows facile charge transfer and thus results in a better cycling performance.

4. CONCLUSION

We reported that EMSA is an efficient electrolyte additive for enhancing the electrochemical performance of a high voltage $LiNi_{0.5}Mn_{1.5}O_4$ cathode. After 500 cycles at 1 C and 25 °C, the $Li/LiNi_{0.5}Mn_{1.5}O_4$ cell with 0.5% EMSA delivered a discharge capacity of 109 mAh g^{-1}, with an improved capacity retention of 84.9%. The cycling performance of the cell with EMSA at 0.5 C and 55 °C was also encouraging, raising the discharge capacity retention from 52.4% to 94.8%. Our studies revealed that EMSA was able to eliminate HF and to enhance the interfacial stability between $LiNi_{0.5}Mn_{1.5}O_4$ and the electrolyte. This unique function of EMSA was essential for the suppression of the undesirable electrolyte decomposition and transition metal ion dissolution, as well as the preservation of the favorable performance of the $LiNi_{0.5}Mn_{1.5}O_4$ cathode. In addition, EMSA showed a positive effect toward the graphite anode, increasing its charge/discharge capacity by approximately 8% throughout the entire 100 cycles. We believe that EMSA, which has the ability to scavenge HF, is a promising additive candidate for improving the cycling performance of lithium ion batteries with a standard carbonate-based electrolyte, especially at elevated temperatures.

ACKNOWLEDGMENTS
This work was financially supported by the National Natural Science Foundation (51574166), and the Scientific and Technological Research and Development Foundation of Shenzhen City (JCYJ20160301145911673).

References

1. R. Santhanam, B. Rambabu, *Journal of Power Sources*, 195 (2010) 5442.
2. J.H. Kim, N.P.W. Pieczonka, L. Yang, *ChemPhysChem*, 15 (2014) 1940.
3. Y.K. Sun, S.T. Myung, B.C. Park, J. Prakash, I. Belharouak, K. Amine, *Nature Materials*, 8 (2009) 320.
4. D. Liu, W. Zhu, J. Trottier, C. Gagnon, F. Barray, A. Guerfi, A. Mauger, H. Groult, C.M. Julien, J.B. Goodenough, K. Zaghi, *RSC Advances*, 4 (2014) 154.
5. H. Duncan, Y. Abu-Lebdeh, I.J. Davidson, *Journal of the Electrochemical Society*, 157 (2010) A528.
6. H. Duncan, D. Duguay, Y. Abu-Lebdeh, I.J. Davidson, *Journal of the Electrochemical Society*, 158 (2011) A537.
7. S. Mai, M. Xu, X. Liao, L. Xing, W. Li, *Journal of Power Sources*, 273 (2015) 816.
8. S.F. Lux, I.T. Lucas, E. Pollak, S. Passerini, M. Winter, R. Kostecki, *Electrochemistry Communications*, 14 (2012) 47.
9. A.V. Plakhotnyk, L. Ernst, R. Schmutzler, *Journal of Fluorine Chemistry*, 126 (2005) 27.
10. K. Tasaki, K. Kanda, S. Nakamura, M. Ue, *Journal of the Electrochemical Society*, 150 (2003) A1628.
11. S.E. Sloop, J.B. Kerr, K. Kinoshita, *Journal of Power Sources*, 119-121 (2003) 330.
12. S.-Y. Ha, J.-G. Han, Y.-M. Song, M.-J. Chun, S.-I. Han, W.-C. Shin, N.-S. Choi, *Electrochimica Acta*, 104 (2013) 170.

13. Y.M. Song, J.G. Han, S. Park, K.T. Lee, N.S. Choi, *Journal of Materials Chemistry A*, 2 (2014) 9506.
14. J.-H. Cho, J.-H. Park, M.-H. Lee, H.-K. Song, S.-Y. Lee, *Energy & Environmental Science*, 5 (2012) 7124.
15. L. Terborg, S. Weber, F. Blaske, S. Passerini, M. Winter, U. Karst, S. Nowak, *Journal of Power Sources*, 242 (2013) 832.
16. Y.-M. Song, C.-K. Kim, K.-E. Kim, S.Y. Hong, N.-S. Choi, *Journal of Power Sources*, 302 (2016) 22.
17. M. Xu, Y. Liu, B. Li, W. Li, X. Li, S. Hu, *Electrochemistry Communications*, 18 (2012) 123.
18. J. Xu, Y. Hu, T. liu, X. Wu, *Nano Energy*, 5 (2014) 67.
19. M. He, L. Hu, Z. Xue, C.C. Su, P. Redfern, L.A. Curtiss, B. Polzin, A. von Cresce, K. Xu, Z. Zhang, *Journal of the Electrochemical Society*, 162 (2015) A1725.
20. L. Xue, S.Y. Lee, Z. Zhao, C.A. Angell, *Journal of Power Sources*, 295 (2015) 190.
21. E. Nanini-Maury, J. Światowska, A. Chagnes, S. Zanna, P. Tran-Van, P. Marcus, M. Cassir, *Electrochimica Acta*, 115 (2014) 223.
22. J. Zhang, S. Fang, L. Qu, Y. Jin, L. Yang, S.-i. Hirano, *Journal of Applied Electrochemistry*, 45 (2015) 235.
23. J. Kalhoff, D. Bresser, M. Bolloli, F. Alloin, J.Y. Sanchez, S. Passerini, *ChemSusChem*, 7 (2014) 2939.
24. M. Nie, B.L. Lucht, *Journal of the Electrochemical Society*, 161 (2014) A1001.
25. Y. Yamada, M. Yaegashi, T. Abe, A. Yamada, *Chemical Communications*, 49 (2013) 11194.
26. F. Wu, Q. Zhu, R. Chen, N. Chen, Y. Chen, L. Li, *Nano Energy*, 13 (2015) 546.
27. N.P.W. Pieczonka, L. Yang, M.P. Balogh, B.R. Powell, K. Chemelewski, A. Manthiram, S.A. Krachkovskiy, G.R. Goward, M. Liu, J.-H. Kim, *The Journal of Physical Chemistry C*, 117 (2013) 22603.
28. Y. Hisayuki, I. Takao, M. Fujita, S. Mitsuru, *Journal of Power Sources*, 99 (2001) 60.
29. Y. Li, R. Zhang, J. Liu, C. Yang, *Journal of Power Sources*, 189 (2009) 685.
30. K. Kim, Y. Kim, E.S. Oh, H.C. Shin, *Electrochimica Acta*, 114 (2013) 387.
31. J. Zheng, J. Xiao, M. Gu, P. Zuo, C. Wang, J.-G. Zhang, *Journal of Power Sources*, 250 (2014) 313.
32. J.G. Han, S.J. Lee, J. Lee, J.S. Kim, K.T. Lee, N.S. Choi, *ACS Applied Materials & Interfaces*, 7 (2015) 8319.
33. M. Dahbi, F. Ghamouss, M. Anouti, D. Lemordant, F. Tran-Van, *Journal of Applied Electrochemistry*, 43 (2013) 375.
34. J. Chen, H. Zhang, M. Wang, J. Liu, C. Li, P. Zhang, *Journal of Power Sources*, 303 (2016) 41.
35. D. Lu, M. Xu, L. Zhou, A. Garsuch, B.L. Lucht, *Journal of the Electrochemical Society*, 160 (2013) A3138.
36. T. Yim, K.S. Kang, J.-S. Yu, K.J. Kim, M.-S. Park, S.-G. Woo, G. Jeong, Y.N. Jo, K.Y. Im, J.-H. Kim, Y.-J. Kim, *Japanese Journal of Applied Physics*, 53 (2014) 08NK01.